Vol.4, No.8, Page 2407- 2415, 2026 https://doi.org/10.59628/jast.v4i8.3246 ISSN 2958-9568 JAST

SUN PUBLISHER

مجلة جامعة صنعاء للعلوم التطبيقية والتكنولوجيا

Sana'a University Journal of Applied Sciences and Technology

https://journals.su.edu.ye/index.php/jast/

Solar-Driven Photocatalytic Degradation of Pharmaceutical Wastewater using ZnO Nanoparticles

Rehab Sh. AL-Selwi[1]*, Anass A. Alnedhary[2] and Mahfoudh M. AL-Hamadi[1]

[1]**Department of Chemistry, Faculty of Science, Sana'a University, Sana'a, Yemen,**
[2]**Department of Chemistry, Faculty of Education, Khawlan Branch, Sana'a University, Sana'a, Yemen**

*Corresponding author: rehab.alselwi@su.edu.ye

Abstract

The increasing discharge of pharmaceutical residues into aquatic environments poses a serious environmental threat due to their persistence and resistance to conventional wastewater treatment processes. In this study, zinc oxide nanoparticles (ZnO NPs) were synthesized via a simple precipitation method and applied as an efficient photocatalyst for the degradation and mineralization of paracetamol under UV irradiation (365 nm) and natural solar irradiation. The structural, optical, and crystalline properties were confirmed using Ultraviolet–Visible Spectrophotometer, Fourier-Transform Infrared Spectroscopy and X-ray Diffraction analyses, revealing high crystallinity and nanoscale features with an average crystallite size ranging between 32.4 and 36.4 nm, which directly facilitated the surface-driven photocatalytic pathway. The results demonstrated that the synthesized ZnO NPs achieved 100% degradation of 10 mg/L paracetamol within 60 min under optimized solar irradiation conditions (pH 11, 2.5 g/L catalyst dose, 600 rpm stirring speed at room temperature). Furthermore, Chemical Oxygen Demand (COD) analysis confirmed complete mineralization of organic content, reducing the initial COD of real wastewater from 21,780 mg/L to 0.5 mg/L, achieving a 99.99% removal efficiency while High-Performance Liquid Chromatography results verified the fully degraded parent compound. A major strength of this study is the utilization of both paracetamol and real pharmaceutical industrial wastewater, which enhances the environmental relevance and practical applicability of the proposed treatment system. The study highlights ZnO NPs as a highly efficient, low-cost, and sustainable photocatalyst for solar-driven wastewater treatment applications, with strong potential for large-scale environmental remediation.

Article Info

Keywords:
ZnO NPs, Photocatalytic degradation, Pharmaceutical Wastewater treatment, Paracetamol.

Article History:
Received: 22-May-2026,
Revised: 26-June-2026,
Accepted: 29-June-2026,
Published: 28 August 2026.

1. INTRODUCTION

The continuous discharge of pharmaceutical residues into aquatic environments has emerged as a serious global environmental concern owing to their persistence, chemical stability, and resistance to conventional wastewater treatment processes [1]. These compounds are widely recognized as emerging contaminants and have been frequently detected in surface water, groundwater, and hospital effluents [2]. Conventional wastewater treatment technologies, including biological degradation [3], adsorption [4], and coagulation–flocculation [5], often exhibit variable and incomplete removal efficiencies for paracetamol, resulting in its continuous release into aquatic environments [6, 7]. Paracetamol was selected as a model pollutant in this study because of its widespread global consumption, high frequency of detection in aquatic systems, and potential to form toxic transformation products if left untreated. Consequently, advanced oxidation processes (AOPs) have gained significant attention as efficient alternative treatment strategies [8]. These processes are based on the in situ generation of highly reactive oxygen species (ROS), particu-

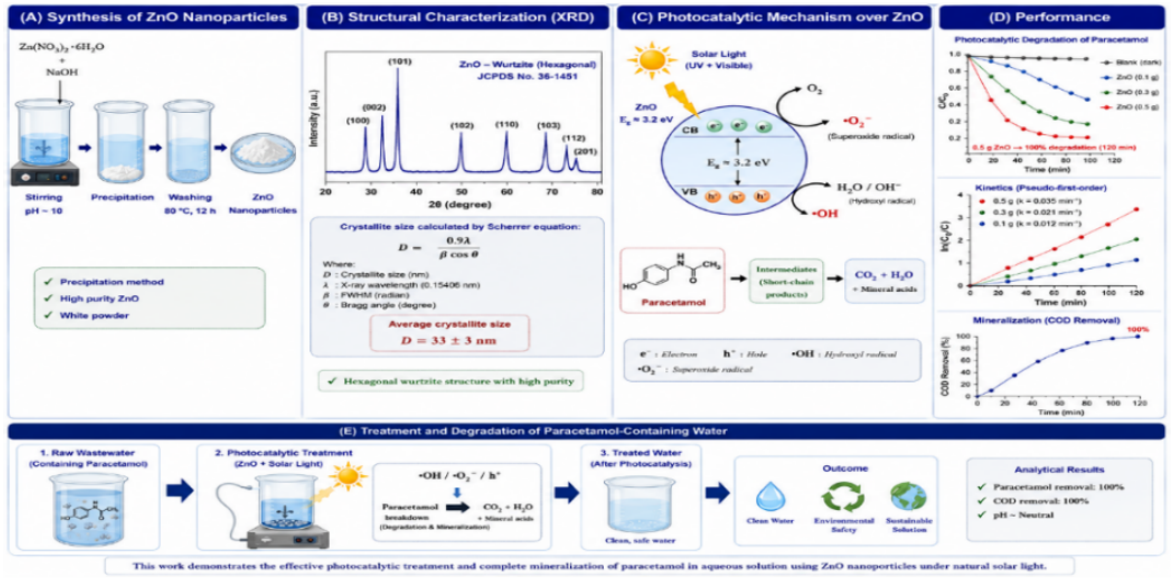

Graph abstract

larly hydroxyl radicals (OH), which non-selectively oxidize organic pollutants and convert them into harmless end-products such as CO_2 and H_2O [9–11].

Among AOPs, heterogeneous photocatalysis using semiconductor materials has emerged as a promising, sustainable, and environmentally friendly approach for water purification, particularly under solar irradiation [12]. Upon exposure to photons with energy equal to or greater than the bandgap, electrons are excited from the valence band (VB) to the conduction band (CB), generating electron–hole (e^-/h^+) pairs [13, 14].

ZnO NPs are among the most extensively studied semiconductor photocatalysts because of their wide bandgap (∼3.37 eV), high exciton binding energy, chemical stability, low cost, and environmental compatibility [15]. However, their photocatalytic efficiency is highly dependent on the particle size, crystallinity, surface area, and defect density [16–19].

Recent studies have reported the effectiveness of ZnO NPs in the photocatalytic degradation of paracetamol under various synthesis methods and irradiation conditions [20, 21]. Green-synthesized ZnO NPs have demonstrated removal efficiency up to 96.8% under optimized conditions [22], while polyol-derived ZnO NPs showed significant degradation under UV-LED irradiation [23]. However, most of these studies have focused on artificial UV irradiation and synthetic wastewater systems, with limited attention to solar-driven photocatalysis under real wastewater conditions.

Therefore, the major strength and novelty of this study is the evaluation of the synthesized ZnO NPs for paracetamol degradation utilizing both a synthetic matrix and real high-strength pharmaceutical industrial wastewater collected from a manufacturing plant. This choice significantly enhanced the environmental relevance, practical applicability, and scalability of the proposed solar-driven treatment system.

2. MATERIALS AND METHODS

2.1. Chemicals and Reagents

Paracetamol was obtained as a pharmaceutical-grade compound from a certified pharmaceutical supplier and used without purification. Zinc nitrate hexahydrate ($Zn(NO_3)_2$ $6H_2O$, ≥98%, BDH) was used as the zinc precursor for the synthesizing of ZnO NP. Sodium hydroxide (analytical grade, ≥98%, BDH) was used as a precipitating agent. Stock solutions of (NaOH 2.0 M) were systematically prepared using deionized water (DIW) for all synthesis and dilution procedures. pH adjustment was performed during the synthesis. All chemicals were of analytical grade and used as received, without further purification.

2.2. Preparation of ZnO NP

ZnO NP were synthesized via chemical precipitation. Zinc nitrate hexahydrate (0.122 mol) was dissolved in deionized water (DIW) under continuous stirring (IKA C-MAG HS 7, Germany) at 80–90 °C. The pH (Plintest PT1330 MICRO 800 PH Meter, United Kingdom) of the solution was adjusted to 11 using an NaOH solution and continuously stirred (∼600 rpm) to ensure complete precipitation. The resulting white precipitate was aged for 1 h, followed by centrifugation at 4500 rpm for 30 min to isolate the white precipitate efficiently and repeated washing with DIW until a neutral pH was achieved. The product was then dried at 160 °C for 12 h (Memmert UN55, Germany) and calcined at 600 °C for 3 h (Nabertherm L 9/11 B180, Germany) to obtain calcined crystalline ZnO NP. Ultrasonic treatment (Branson B-5200 E4, USA) operating at a fixed frequency of 40 kHz

and an acoustic power output of 120 W was applied during washing to improve dispersion and remove residual ions [24].

2.3. Characterization Techniques

The optical properties of ZnO NP were analyzed using UV–Vis spectrophotometry (Specord 200, Analytic Jena, Germany) in the wavelength range of 200–600 nm. The bandgap energy was estimated using Tauc's relation: Functional groups were identified using Fourier Transform Infrared Spectroscopy (FTIR, 410, JASCO, Japan) in the range 4000–400 cm^{-1}. The crystalline structure and phase purity were analyzed using X-ray diffraction (XRD, 9800 XP SIM-SEQ XRF OF (Amran Cement Plant). The average crystallite size was calculated using the Debye–Scherrer Equation based on the most intense diffraction peak [25].

2.4. Photocatalytic Degradation Experiments

Photocatalytic experiments were conducted in batch mode under UV irradiation (365 nm, Vilber Lourmat, France) and natural sunlight. A known amount of ZnO NP (0.1–0.25 g) was dispersed in 100 ml of paracetamol solution with different initial concentrations (10, 50, and 100 mg/L). Prior to irradiation, the suspension was magnetically stirred in the dark for 30 min to establish adsorption–desorption equilibrium. At regular time intervals, aliquots were collected, centrifuged to remove catalyst particles, and the remaining concentration of paracetamol was analyzed using UV–Vis spectrophotometry at $\lambda_{max} = 243$ nm. As shown in Figure 4, the degradation efficiency was calculated by difference using Equation Eq. (1).

$$\text{Degradation Efficiency} = \frac{C_0 - C_t}{C_0} \times 100 \qquad (1)$$

where C_0 is the initial concentration and C_t is the concentration at time t.

All batch degradation tests and chemical measurements were performed under optimized environmental conditions, and the data points were reported based on direct experimental monitoring. Experimental plotting, data processing, and pseudo-first-order kinetic linear fittings were systematically performed using Microsoft Excel.

2.5. Chemical Oxygen Demand (COD) Measurement

COD was measured according to the standard methods for water and wastewater analysis [26]. The COD removal efficiency (COD_{RE}) was calculated using Equation Eq. (2).

$$COD_{RE} = \frac{COD_0 - COD_t}{COD_0} \times 100 \qquad (2)$$

where COD_0 and COD_t represent initial and final COD_{RE} values, respectively.

2.6. High-Performance-Liquid Chromatography (HPLC) Analysis

HPLC analysis was performed using a Waters e2695 Alliance system (Waters, USA) equipped with a UV/Vis detector and an auto-sampler. Separation was achieved using an XB-C18 reversed-phase column (15 cm × 4.6 mm, 5 μm). The mobile phase consisted of 0.05 M KH_2PO_4 (A) and 10% acetonitrile (B) under elution. The flow rate was set to 1.0 ml/min. Detection was performed at 220 and 254 nm. The injection volume was maintained at 1 μL.

3. RESULTS AND DISCUSSION

3.1. Quantitative Yield of ZnO NP

ZnO NP were successfully synthesized via a chemical precipitation method under controlled conditions. A high production yield of 9.31 g (93.1%) was obtained from a theoretical yield of 10.00 g. This high conversion efficiency indicates the effective transformation of precursor materials into ZnO NP and confirms the reliability and reproducibility of the precipitation-based synthesis route.

3.2. Characterization of ZnO NP

The synthesized ZnO NPs were systematically characterized using UV–Vis., FTIR, and XRD to investigate their optical, chemical, and structural properties.

3.2.1. UV–Vis Spectrophotometric Analysis

The UV–Vis absorption spectra of ZnO NP exhibited a strong absorption band in the ultraviolet region at $\lambda_{max} = 378$ nm, confirming their semiconductor nature and successful formation. A distinct absorption edge was observed at approximately 378 nm, indicating the optical response of the ZnO NP in the UV region. The bandgap energy was estimated to be approximately 3.4 eV, as shown in Figure 1 using Tauc plot analysis [27],

$$(\alpha h\nu)^n = A(h\nu - E_g) \qquad (3)$$

which is consistent with previously reported values for ZnO nanostructures [20]. The observed optical behavior suggests the presence of nanoscale effects and confirms the suitability of the synthesized ZnO NP for photocatalytic applications.

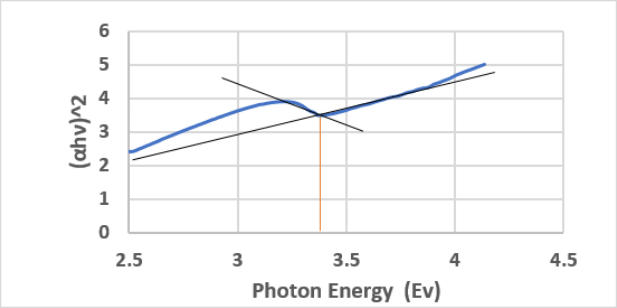

Figure 1. Tauc plot to determine the bandgap for ZnO NP.

3.2.2. FTIR Spectroscopic Analysis

The FTIR spectrum of ZnO NP was recorded in the range of 4000–400 cm^{-1} to identify the functional groups and confirm the chemical bonding. A characteristic absorption band observed in the range of 450–500 cm^{-1} was attributed to Zn–O stretching vibrations, confirming the successful formation of ZnO NP [28].

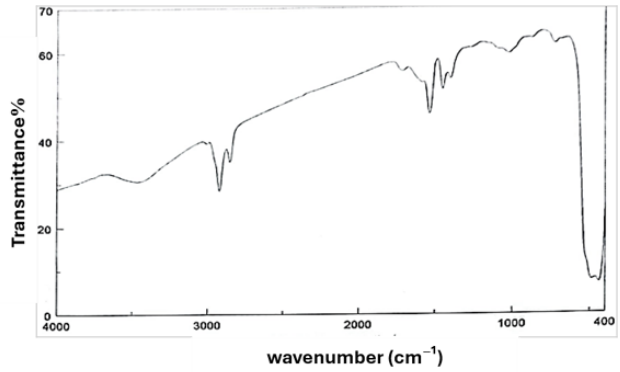

Figure 2. FTIR spectrum of ZnO NP.

3.2.3. X-ray Diffraction (XRD) Analysis

XRD analysis confirmed the crystalline structure and phase purity of the ZnO NP samples. The sharp diffraction peaks in Figure 3 indicate the high crystallinity of the synthesized ZnO NPs. The diffraction profile of the calcined ZnO nanoparticles is indexable to the standard hexagonal wurtzite phase (JCPDS card no. 36-1451), showing characteristic peaks corresponding to the lattice planes of (100), (002), (101), (102), (110), (103), and (112). The average crystallite size of the synthesized ZnO NP was estimated using Equation Eq. (4) [25], and the results are presented in Table 1.

$$D = \frac{k\lambda}{\beta \cos\theta} \tag{4}$$

The estimated crystallite sizes were noticeable, whereas ZnO NP showed smaller crystallite sizes in the range of approximately 32.4–36.4 nm. The reduction in the crystallite size suggests improved nucleation and growth control during synthesis, which contributes to a higher surface area. Therefore, we expected it to exhibit highly enhanced photocatalytic performance.

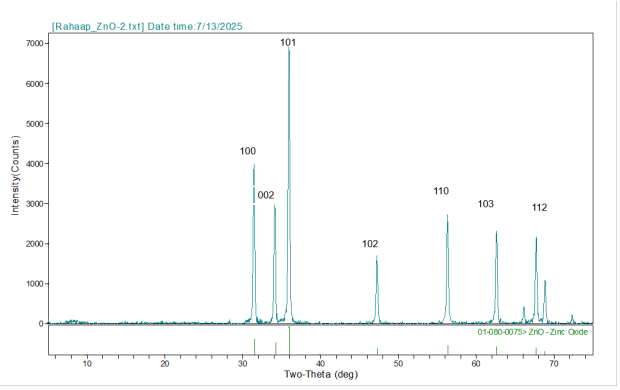

Figure 3. XRD pattern for ZnO NP.

Table 1. Crystallite size of ZnO NP calculated at peaks height > 1000.

2θ	FWHM	Crystallite D (nm)	Average D (nm)
31.441	0.228	36.391	34.538
34.138	0.230	36.074	
35.940	0.247	33.591	
47.221	0.237	35.009	
56.301	0.244	34.005	
62.620	0.256	32.412	
67.738	0.242	34.287	

3.2.4. Multi-Analytical Correlation

The high degradation efficiency was directly driven by the optical and structural synergy of the catalyst. The small crystallite size determined via XRD (32.4–36.4 nm) yields an expanded active surface area with dense catalytic-site density. The UV-Vis profiles show strong photon absorption in the solar spectrum, promoting efficient charge-carrier generation. This underlying mechanism was chemically verified by the rapid decline in the primary UV absorbance peaks and the corresponding disappearance of the parent compound peak in the HPLC chromatograms.

3.3. Optimization of the Parameters Affecting Paracetamol Degradation

The maximum absorption wavelength of paracetamol was determined to be 243 nm using UV–Vis spectrophotometry (Figure 4). This wavelength was selected for all subsequent photocatalytic experiments to ensure accurate and reliable monitoring of the paracetamol degradation under different reaction conditions.

3.3.1. Effect of Irradiation Source on Photocatalytic Degradation

The photocatalytic degradation performance of ZnO NP was evaluated under three different illumination environments: natural solar light, an artificial UV lamp (365 nm), and a dark control (without irradiation). Additionally, a photolysis control experiment (natural solar light with-

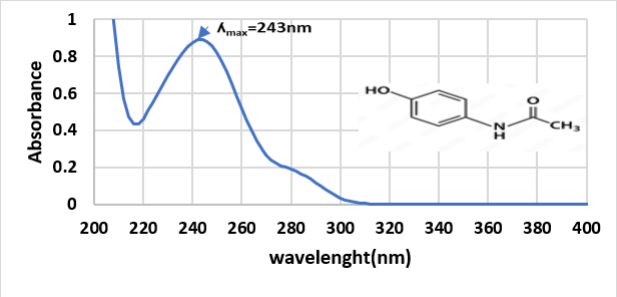

Figure 4. UV-Vis absorption spectrum of standard paracetamol solution.

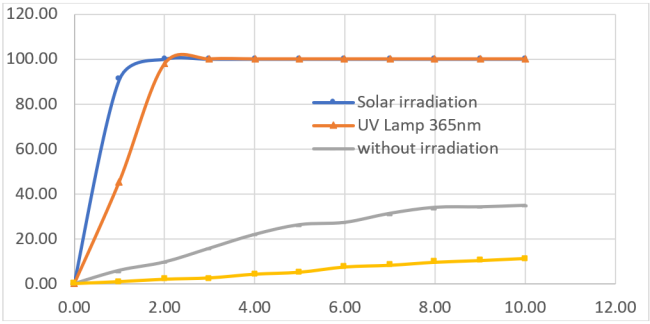

Figure 5. Comparative study of paracetamol degradation: UV, solar, without irradiation conditions and without catalyst.

out the ZnO catalyst) was conducted to establish the baseline degradation rate of paracetamol. For each batch, 0.25 g of ZnO NPs was dispersed in 100 mL of a 10 mg/L standard paracetamol solution under continuous stirring, and the degradation process was monitored at $\lambda_{\max} = 243$ nm. The experimental results, systematically presented in Table 2 and Figure 5, demonstrate a profound dependence of the degradation efficiency on the light source. Under natural solar light, the ZnO NPs exhibited superior photocatalytic activity, achieving 90.85 removal within 1 h and complete 100% degradation at 2 h. Under artificial UV light (365 nm), the system achieved 45.42% degradation at 1 h, reaching completion (100%) after 3 h. Conversely, the dark control (without irradiation) exhibited a nominal concentration drop, reaching only 34.82 after a prolonged duration of 10 h. Most importantly, the photolysis control experiment (without catalyst) exhibited negligible degradation, reaching only 11.12% after 10 h, which firmly establishes the baseline stability of paracetamol under solar light in the absence of a photocatalyst.

This profile confirms that photon irradiation is indispensable for generating electron–hole (e^-/h^+) pairs and activating the photocatalytic cycle of the material. The accelerated degradation rate observed under direct natural sunlight compared to that under artificial monochromatic UV exposure is attributed to the full polychromatic solar spectrum. The presence of high-intensity ambient solar radiation induces enhanced thermal energetic states and multiple electronic transitions, thus generating a higher density of localized reactive hydroxyl radicals (OH) [29]. Meanwhile, the progressive concentration drop observed under dark control conditions over 10 h is ascribed to a prolonged physical surface-diffusion-controlled adsorption equilibrium on the nanoparticle surface defects, as no photolytic transformation occurs in the dark. The minimal degradation observed in the absence of the catalyst confirms that the rapid removal of paracetamol is purely driven by a synergistic photocatalytic mechanism rather than direct photolysis.

To rigorously quantitatively validate these findings, the experimental data points were mathematically modeled using the Langmuir–Hinshelwood pseudo-first-order kinetic framework:

$$\ln \frac{C_0}{C_t} = kt \tag{5}$$

The calculated apparent rate constants (k) and their corresponding coefficients of determination (R^2) are listed in Table 3. Natural solar irradiation delivered a superior rate constant of 0.054 min^{-1} (3.2414 h^{-1}) with an excellent linear correlation ($R^2 = 0.9831$), which is significantly faster than that of the artificial UV lamp (0.0399 min^{-1}, $R^2 = 0.9371$). Simultaneously, the dark adsorption control displayed a negligible rate constant (0.0008 min^{-1}, $R^2 = 0.9577$). Importantly, the photolysis control experiment (without catalyst) exhibited the lowest degradation kinetics, with a rate constant of 0.0002 min^{-1} (0.0118 h^{-1}) and a high linear fit ($R^2 = 0.9950$). This quantitative discrepancy further reinforces the conclusion that the degradation of paracetamol is driven solely by the photocatalytic action of ZnO NPs rather than by self-photolysis.

3.3.2. Effect of Stirring Conditions on Paracetamol Degradation

The effect of magnetic stirring (600 rpm) on the photocatalytic degradation of paracetamol was evaluated under solar irradiation using 0.25 g of ZnO NP in 100 mL of a 10 mg/L standard paracetamol solution. As shown in Figure 6, complete degradation was achieved within 1 h under stirring, whereas a significantly longer time was required without the catalyst.

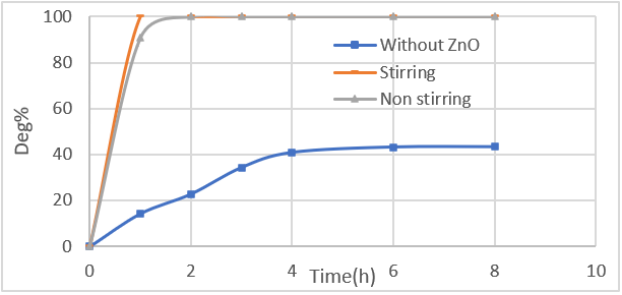

Figure 6. Effect of stirring conditions on paracetamol degradation.

Table 2. Effect of UV and Solar irradiation on degradation efficiency.

Time (h)	Without catalyst	Without irradiation	UV Lamp 365 nm	Solar irradiation
0.00	0.00	0.00	0.00	0.00
1.00	0.85	5.92	45.42	90.85
2.00	1.92	9.60	97.77	100.00
3.00	2.50	15.74	100.00	100.00
4.00	4.15	21.88	100.00	100.00
5.00	5.02	26.23	100.00	100.00
6.00	7.35	27.23	100.00	100.00
7.00	8.10	31.25	100.00	100.00
8.00	9.45	33.93	100.00	100.00
9.00	10.20	34.15	100.00	100.00
10.00	11.12	34.82	100.00	100.00

Table 3. Influence of irradiation source on paracetamol degradation efficiency and pseudo-first-order kinetic parameters.

Irradiation Source	Degradation % (after 10 h)	k (h^{-1})	k (min^{-1})	R^2
Natural Solar	100% (at 2 h)	3.2414	0.054	0.9831
UV Lamp (365 nm)	100% (at 3 h)	2.3921	0.0399	0.9371
Without Irradiation (Dark)	34.82%	0.0453	0.0008	0.9577
Without catalyst	11.12%	0.0118	0.0002	0.9950

3.3.3. Effect of ZnO NP Dose

The effect of ZnO NP dosage on paracetamol degradation was evaluated by varying the catalyst amount (0.1 and 0.25 g) in 100 mL of a 10 mg/L solution under direct solar irradiation without stirring. As shown in Table 4, increasing the catalyst dosage significantly enhanced the degradation rate. Complete degradation was achieved using 0.25 g of ZnO NPs, whereas a lower dosage (0.1 g) required 4 h to achieve complete degradation. The enhanced performance at higher catalyst loadings can be attributed to the increased number of active surface sites available for photon absorption and reactive species generation, leading to faster pollutant breakdown.

Table 4. Effect of catalyst dose on paracetamol degradation.

Time (h)	0.1 g		0.25 g	
	Abs	Deg%	Abs	Deg%
0	0.9	0	0 .9	0
1	0.34	62.11	0.08	90.81
2	0.14	84.42	0	100
3	0.06	92.94	0	100
4	0	100	0	100
5	0	100	0	100
6	0	100	0	100
7	0	100	0	100

3.3.4. Effect of Initial Concentration of Paracetamol on Degradation Efficiency

The influence of initial paracetamol concentration (10, 50, and 100 mg/L) on the photocatalytic degradation was investigated using 0.25 g of ZnO NP in 100 ml solution under solar irradiation with stirring. The results in Table 4 reveal that complete degradation of 10 mg/L was achieved within only 1 h whereas 50 mg/L required 4 h but required up to 7 h for a concentration of 100 mg/L. As shown in Table 4, complete degradation of paracetamol at an initial concentration of 10 mg/L was achieved within 1 h. In contrast, complete degradation required 4 h and 7 h for initial concentrations of 50 mg/L and 100 mg/L, respectively. The 100 mg/L paracetamol target was confirmed to be fully dissolved, sitting well below the established aqueous solubility limit (∼14,000 mg/L). Pseudo-first-order rate constants (k, min^{-1}) were calculated for each concentration profile to provide a quantitative validation.

Table 5. Influence of initial concentration on paracetamol degradation efficiency and pseudo-first-order kinetic parameters.

Initial Concentration (mg/L)	Time for 100% Degradation (h)	Rate Constant k(h^{-1})	Rate Constant k (min^{-1})	R^2
10	1	6.5436	0.1091	0.9999
50	4	2.1531	0.0359	0.8684
100	7	1.3196	0.022	0.9578

To rigorously quantitatively validate the concentration dependence, the experimental data profiles were mathematically modeled using the Langmuir–Hinshelwood pseudo-first-order kinetic framework. The calculated apparent rate constants (k) and their corresponding coefficients of determination (R^2) are systematically organized across the different concentration gradients in Table 4. Kinetic analysis revealed a clear inverse relationship between the initial pollutant concentration and degradation rate constant. The rate decreased substantially from (0.1091 min^{-1}) at 10 mg/L to k = 2.1531 h^{-1} (0.0359 min^{-1}) at 50 mg/L, and further dropped to k = 1.3196 h^{-1} (0.0220 min^{-1}) when the initial paracetamol concentration was increased to 100 mg/L. This decline in the apparent rate is primarily governed by the competitive occupation of the available active photocatalytic sites on the surface of the ZnO NPs. At elevated initial concentrations, an excessive number of parent paracetamol molecules and their primary intermediate degradation products accumulated on the catalyst surface, causing

saturation and restricting the direct interaction between photons and active sites. Furthermore, increasing the solute concentration yields a more optically dense reaction-fluid matrix. This density induces a "UV-screening" or shading effect that curtails nominal photon penetration depth through the solution, thereby decreasing the absolute production rate of reactive oxygen species (ROS) and hydroxyl radicals (OH).

The photocatalytic degradation of paracetamol was confirmed using chemical oxygen demand (COD) and HPLC analyses. COD values decreased from 127 mg/L to 0 mg/L, indicating 100% removal efficiency and complete mineralization. This confirms the high efficiency of the ZnO NP under sunlight with continuous stirring. HPLC analysis showed a paracetamol peak at 10.543 min (Figure 7), which disappeared after treatment, confirming efficient degradation. New peaks at lower retention times indicate the presence of intermediate products. Overall, the COD and HPLC results confirmed the effective degradation and progressive mineralization of paracetamol under the applied conditions.

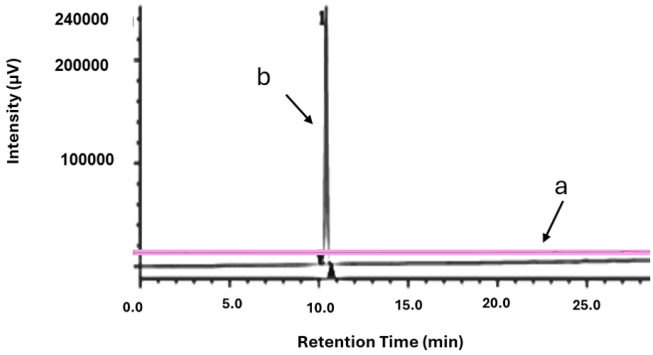

Figure 7. HPLC chromatogram of paracetamol: (a) before, (b) after.

3.3.5. Photocatalytic Stability Study

The catalytic stability and reaction profile of the synthesized ZnO NPs were investigated over a 5-hour photocatalytic degradation period under optimized conditions to evaluate their potential for practical applications. As summarized in Table 6, the ZnO NPs demonstrated highly efficient and progressive performance against paracetamol. The catalyst achieved an outstanding degradation efficiency of 82.20% within only 5 hours. The kinetic profile maintained a steady and uninterrupted generation of reactive oxygen species (ROS) without sudden deceleration or premature catalyst deactivation. This robust performance over a 5-hour duration indirectly reflects the excellent crystalline stability and structural integrity of the ZnO NPs, confirming their suitability for treating persistent pharmaceutical pollutants.

Table 6. Reusability and degradation efficiency of paracetamol using ZnO NPs.

Time (h)	0	3	5
Degradation Efficiency (%)	0	29.95	82.2

3.4. Treatment of Real Pharmaceutical Wastewater with ZnO NP

Before evaluating the degradation efficiency of the pharmaceutical wastewater sample using ZnO NP, the selection of an appropriate analytical wavelength was essential to ensure accurate monitoring of the photocatalytic process. Given the complex matrix of real wastewater, which may contain multiple pharmaceutical residues and potentially interfering substances, careful wavelength selection is required to obtain reliable absorbance measurements during degradation. The UV–Vis spectrum of the untreated sample, as presented in Figure 8, revealed two distinct absorption maxima at 330 and 520 nm. These wavelengths were therefore selected as reference points and used as baseline indicators for monitoring changes in absorbance throughout the degradation process. Real industrial wastewater samples were collected directly from the primary equalization tank of a local pharmaceutical manufacturing facility in Sana'a, Yemen, explaining the characteristically dense initial COD load (21,780 mg/L).

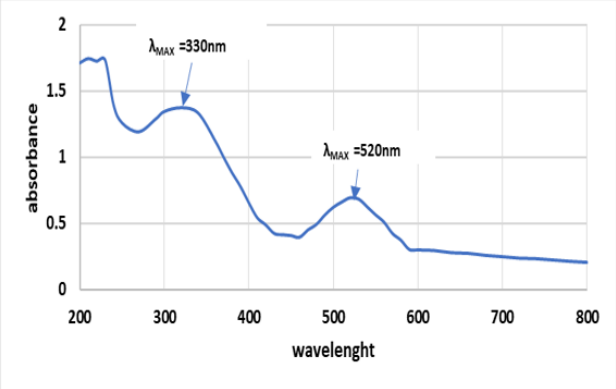

Figure 8. UV-VIS absorption spectrum of pharmaceuticals wastewater.

To study the effectiveness of ZnO NP on the photocatalytic degradation of pharmaceutical wastewater, 0.1 g of ZnO NP was added to 10 mL of pharmaceutical wastewater samples (yielding a catalyst loading of 10 g/L) exposed to solar irradiation with stirring for various time intervals. A higher catalyst loading of 10 g/L was utilized for the real industrial matrix to overcome competitive adsorption from non-target organic fractions and to compensate for the reduced optical path caused by the high initial turbidity of the effluent.

The degradation percentage was monitored by measuring the absorbance at 330 nm and 520 nm at different

time intervals, and the obtained results are summarized in Table 7. Consequently, this system demonstrates outstanding potential as a highly suitable catalyst treatment strategy for pharmaceutical effluents. Monitoring at 330 nm tracks the aromatic core decomposition of parent active pharmaceutical ingredients (APIs), whereas tracking at 520 nm corresponds to the continuous decolorization of auxiliary chromophoric compounds present in the complex effluent. The treated matrix showed a notable decrease in the characteristic absorption peaks associated with the pharmaceutical compounds. The reduction in absorbance confirmed the partial or complete disappearance of the parent molecules, indicating effective photocatalytic degradation.

Table 7. Effect of ZnO NP on pharmaceutical degradation.

Time (h)	Degradation % (530 nm)	Degradation % (320 nm)
0	0.00	0.00
1	7.69	35.00
2	15.38	60.00
3	46.15	78.00
4	81.54	92.00
5	95.38	100.00
6	100.00	100.00

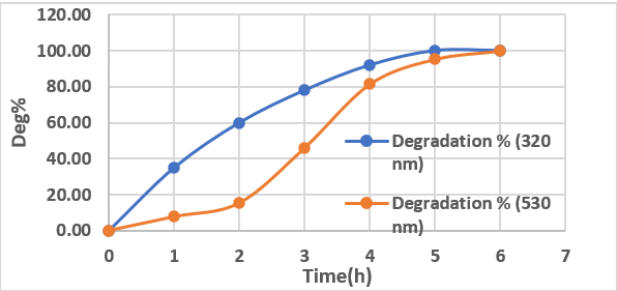

Figure 9. Effect of ZnO NP on pharmaceutical degradation.

To evaluate the efficiency of the photocatalytic degradation process applied to real pharmaceutical wastewater, COD analyses were performed before and after treatment. The initial pH of the raw effluent was 7.4, and it shifted to approximately 6.8 after the 6-hour solar treatment cycle due to the transient generation of acidic intermediate transformation products. The results revealed a complete elimination of organic load, as the COD value decreased from 21780 mg/L before treatment to 0.5 mg/L after photocatalytic irradiation, corresponding to achieving a 99.99% removal efficiency. This substantial reduction, verified via systematic matrix dilutions to ensure measurement accuracy, confirms the high mineralization capability of the optimized ZnO photocatalytic system and its proficiency in converting complex industrial contaminants into benign inorganic end-products (CO_2 and H_2O).

4. CONCLUSION

In summary, crystalline ZnO NPs (32.4–36.4 nm) synthesized via precipitation exhibited excellent photocatalytic performance, achieving 100% degradation of paracetamol within 1.0 h under optimized solar conditions (2.5 g/L catalyst, pH 11). The kinetic profiles followed a pseudo-first-order model dominated by hydroxyl radicals (OH). The system demonstrated strong real-world application by successfully mineralizing a high-strength industrial pharmaceutical effluent (21,780 mg/L COD) within 6.0 h under natural sunlight. Future research should focus on pilot-scale continuous reactor design and fixed-bed immobilization to minimize catalyst recovery stages.

DECLARATIONS

Ethical Approval

This article does not contain any studies involving animals or human participants performed by any of the authors. We declare that this manuscript is original and is not currently considered for publication elsewhere. We further confirm that the order of authors listed in the manuscript has been approved by all of us.

Conflict of interest

The authors declare no competing interests.

Competing interests

The authors have no financial or proprietary interest in any material discussed in this article.

Authors' contributions

All authors contributed to the conception and design of the study. All authors performed simulations, data collection and analysis, and commented on the present version of the manuscript. All the authors have read and approved the final manuscript.

Funding

No funding was received from any organization for this study.

Availability of data and materials

No datasets is used in the present study.

Consent for publication

The authors confirm that informed consent was obtained for the publication of the data contained in this article.

Consent to participate

Informed consent was obtained from all authors.

REFERENCES

[1] D. Fatta-Kassinos, S. Meric, and A. Nikolaou, "Pharmaceutical residues in environmental waters and wastewater: Current state of knowledge and future research," *Anal. Bioanal. Chem.*, vol. 399, no. 1, pp. 251–275, 2011. DOI: 10.1007/s00216-010-4300-9

[2] I. O. Sanusi, G. O. Olutona, I. G. Wawata, and H. Onohuean, "Occurrence, environmental impact and fate of pharmaceuticals in groundwater and surface water: A critical review," *Environ. Sci. Pollut. Res.*, vol. 30, pp. 90 595–90 614, 2023. DOI: 10.1007/s11356-023-28802-4

[3] P. Ranjit, V. Jhansi, and K. V. Reddy, "Conventional wastewater treatment processes," in *Advances in the Domain of Environmental Biotechnology: Environmental and Microbial Biotechnology*, N. R. Maddela, L. C. García Cruzatty, and S. Chakraborty, Eds., Singapore: Springer, 2021. DOI: 10.1007/978-981-15-8999-7_17

[4] A. Dąbrowski, "Adsorption—from theory to practice," *Adv. Colloid Interface Sci.*, vol. 93, no. 1-3, pp. 135–224, 2001. DOI: 10.1016/S0001-8686(00)00082-8

[5] C. Zhao et al., "Application of coagulation/flocculation in oily wastewater treatment: A review," *Sci. Total. Environ.*, vol. 765, p. 142 795, 2021. DOI: 10.1016/j.scitotenv.2020.142795

[6] W. J. Lee, P. S. Goh, W. J. Lau, C. S. Ong, and A. F. Ismail, "Removal of pharmaceutical contaminants from aqueous medium: A state-of-the-art review based on paracetamol," *Arab. J. for Sci. Eng.*, vol. 45, pp. 7109–7135, 2020. DOI: 10.1007/s13369-020-04446-1

[7] W. H. A. Edrees, Q. Y. M. Abdullah, A. G. AL-Kaf, and K. M. Naji, "A review on comparative study between physicochemical and biological processes for paracetamol degradation," *Univers. J. Pharm. Res.*, vol. 2, no. 4, pp. 24–29, 2017.

[8] Y. Deng and R. Zhao, "Advanced oxidation processes (aops) in wastewater treatment," *Curr. Pollut. Reports*, vol. 1, no. 3, pp. 167–176, 2015. DOI: 10.1007/s40726-015-0015-z

[9] M. Dai, Q. Niu, S. Wu, Y. Lin, and S. Zhou, "Hydroxyl radicals in ozone-based advanced oxidation of organic contaminants: A review," *Environ. Chem. Lett.*, vol. 22, no. 6, pp. 3059–3106, 2024. DOI: 10.1007/s10311-024-01772-w

[10] M. Y. D. Alazaiza, T. M. Alzghoul, O. Farobie, A.-N. Al-Yazeedi, S. S. Abu Amr, and M. J. K. Bashir, "Advanced oxidation processes in water treatment: Mapping 15 years of scientific progress and collaboration," *Environments*, vol. 13, no. 2, p. 103, 2026. DOI: 10.3390/environments13020103

[11] K. H. H. Aziz, F. S. Mustafa, M. A. H. Karim, and S. Hama, "Pharmaceutical pollution in the aquatic environment: Advanced oxidation processes as efficient treatment approaches: A review," *Mater. Adv.*, vol. 6, no. 11, pp. 3433–3454, 2025. DOI: 10.1039/D4MA01122H

[12] H. Liu, C. Wang, and G. Wang, "Photocatalytic advanced oxidation processes for water treatment: Recent advances and perspective," *Chem. - An Asian J.*, vol. 15, no. 20, pp. 3239–3253, 2020. DOI: 10.1002/asia.202000895

[13] Q. Shao, H. Lin, and M. Shao, "Determining locations of conduction bands and valence bands of semiconductor nanoparticles based on their bandgaps," *ACS Omega*, vol. 5, no. 18, pp. 10 297–10 300, 2020. DOI: 10.1021/acsomega.9b04238

[14] A. N. Tuama, L. H. Alzubaidi, M. H. Jameel, K. H. Abass, M. Z. H. bin Mayzan, and Z. N. Salman, "Impact of electron-hole recombination mechanism on the photocatalytic performance of zno in water treatment: A review," *J. Sol-Gel Sci. Technol.*, vol. 110, no. 3, pp. 792–806, 2024. DOI: 10.1007/s10971-024-06385-x

[15] M. S. Samuel, L. Bose, and K. C. George, "Optical properties of zno nanoparticles," *Acad. Rev.*, vol. 16, pp. 57–65, 2009.

[16] K. Chen, Q. Fan, C. Chen, Z. Chen, A. Alsaedi, and T. Hayat, "Insights into the crystal size and morphology of photocatalysts," *J. Colloid Interface Sci.*, vol. 538, pp. 638–647, 2019. DOI: 10.1016/j.jcis.2018.12.039

[17] S. Raha and M. Ahmaruzzaman, "Zno nanostructured materials and their potential applications: Progress, challenges and perspectives," *Nanoscale Adv.*, vol. 4, no. 8, pp. 1868–1925, 2022. DOI: 10.1039/D1NA00880C

[18] S. G. Kumar and K. K. Rao, "Zinc oxide based photocatalysis: Tailoring surface-bulk structure and related interfacial charge carrier dynamics for better environmental applications," *RSC Adv.*, vol. 5, no. 5, pp. 3306–3351, 2015. DOI: 10.1039/C4RA13299H

[19] Y. Sun et al., "The applications of morphology controlled zno in catalysis," *Catalysts*, vol. 6, no. 12, p. 188, 2016. DOI: 10.3390/catal6120188

[20] A. Solmaz, T. Turna, and A. Baran, "Removal of paracetamol from aqueous solution with zinc oxide nanoparticles obtained by green synthesis from purple basil (ocimum basilicum l.) waste," *Biomass Convers. Biorefinery*, vol. 14, no. 9, pp. 10 771–10 789, 2024. DOI: 10.1007/s13399-024-05355-1

[21] Y. Li, W. Zhang, J. Niu, and Y. Chen, "Surface-coating-dependent dissolution, aggregation, and reactive oxygen species (ros) generation of silver nanoparticles under different irradiation conditions," *Environ. Sci. & Technol.*, vol. 47, no. 18, pp. 10 293–10 301, 2013. DOI: 10.1021/es400945v

[22] E. D. M. Isa, K. Shameli, H. J. Ch'ng, N. W. C. Jusoh, and R. Hazan, "Photocatalytic degradation of selected pharmaceuticals using green fabricated zinc oxide nanoparticles," *Adv. Powder Technol.*, vol. 32, no. 7, pp. 2398–2409, 2021. DOI: 10.1016/j.apt.2021.05.021

[23] A. Zakiyah, G. R. Anindika, and Y. Kusumawati, "Synthesis of zinc oxide (zno) nanoparticles by polyol method and its application on photocatalytic reduction of paracetamol concentration," in *AIP Conference Proceedings*, vol. 2349, 2021, p. 020 053. DOI: 10.1063/5.0051714

[24] H. R. Ghorbani, F. Parsa Mehr, H. Pazoki, and B. M. Rahmani, "Synthesis of zno nps by precipitation method," *Orient. J. Chem.*, vol. 31, no. 2, pp. 1219–1221, 2015. DOI: 10.13005/ojc/310281

[25] F. T. L. Muniz, M. R. Miranda, C. Morilla dos Santos, and J. M. Sasaki, "The scherrer equation and the dynamical theory of x-ray diffraction," *Acta Crystallogr. Sect. A: Found. Adv.*, vol. 72, no. 3, pp. 385–390, 2016. DOI: 10.1107/S205327331600365X

[26] M. F. Romadhan, N. E. Suyatma, and F. M. Taqi, "Synthesis of zno nanoparticles by precipitation method with their antibacterial effect," *Indonesian J. Chem.*, vol. 16, no. 2, pp. 117–123, 2016. DOI: 10.22146/ijc.21153

[27] J. Tauc, R. Grigorovici, and A. Vancu, "Optical properties and electronic structure of amorphous germanium," *Phys. Status Solidi (b)*, vol. 15, no. 2, pp. 627–637, 1966. DOI: 10.1002/pssb.19660150224

[28] S. U. Geetha and S. Thilakavathy, "Ftir and xrd of zinc oxide nanoparticle from mangifera indica l. anacardiaceae," *J. Pharm. Res. Int.*, vol. 33, no. 47A, pp. 176–181, 2021. DOI: 10.9734/JPRI/2021/v33i47A33001

[29] M. Pelaez et al., "A review on the visible light active titanium dioxide photocatalysts for environmental applications," *Appl. Catal. B: Environ.*, vol. 125, pp. 331–349, 2012. DOI: 10.1016/j.apcatb.2012.05.036